

## Model calculation for enhancement factor of a gated field emission nanotube

D. Lei, L. Y. Zeng, W. B. Wang, and J. Q. Liang

Citation: *J. Appl. Phys.* **102**, 114503 (2007); doi: 10.1063/1.2818019

View online: <http://dx.doi.org/10.1063/1.2818019>

View Table of Contents: <http://jap.aip.org/resource/1/JAPIAU/v102/i11>

Published by the [American Institute of Physics](#).

---

### Related Articles

Effects of lateral and substrate constraint on the piezoresponse of ferroelectric nanostructures  
*Appl. Phys. Lett.* **101**, 112901 (2012)

First-principles study of O-BN: A sp<sup>3</sup>-bonding boron nitride allotrope  
*J. Appl. Phys.* **112**, 053518 (2012)

Morphology dependence of radial elasticity in multiwalled boron nitride nanotubes  
*Appl. Phys. Lett.* **101**, 103109 (2012)

Enhanced Raman scattering and photoluminescence of Bi<sub>3.25</sub>La<sub>0.75</sub>Ti<sub>3</sub>O<sub>12</sub> nanotube arrays for optical and ferroelectric multifunctional applications  
*Appl. Phys. Lett.* **101**, 081903 (2012)

First-principles study of hydrogenated carbon nanotubes: A promising route for bilayer graphene nanoribbons  
*Appl. Phys. Lett.* **101**, 033105 (2012)

---

### Additional information on J. Appl. Phys.

Journal Homepage: <http://jap.aip.org/>

Journal Information: [http://jap.aip.org/about/about\\_the\\_journal](http://jap.aip.org/about/about_the_journal)

Top downloads: [http://jap.aip.org/features/most\\_downloaded](http://jap.aip.org/features/most_downloaded)

Information for Authors: <http://jap.aip.org/authors>

## ADVERTISEMENT



Special Topic Section:  
**PHYSICS OF CANCER**

Why cancer? Why physics? [View Articles Now](#)

## Model calculation for enhancement factor of a gated field emission nanotube

D. Lei, L. Y. Zeng, and W. B. Wang<sup>a)</sup>

Laboratory of Excited-state Processes, Changchun Institute of Optics, Fine Mechanics and Physics, Chinese Academy of Sciences, Changchun 130033, People's Republic of China  
and Graduate School of Chinese Academy of Sciences, Beijing 100039, People's Republic of China

J. Q. Liang

State Key Laboratory of Applied Optics, Changchun Institute of Optics, Fine Mechanics and Physics, Chinese Academy of Sciences, Changchun 130033, People's Republic of China

(Received 20 June 2007; accepted 4 October 2007; published online 4 December 2007)

The field enhancement factor of gated nanotube with opened top was analytically calculated by the electrostatic method. The effect of geometrical parameters of the device on their field enhancement factor was investigated, including the gate-hole radius, gate-anode distance, and nanotube radius. The theoretical analysis shows that the enhancement factor increases greatly with the decrease of gate-hole radius. However, if the gate voltage is zero, the factor increases with the increase of gate-hole radius, and finally reaches a constant, which increases with the increase of nanotube length  $L$ . The enhancement factor  $\beta$  gets larger when the nanotube radius gets smaller. As the gate-anode distance  $d_2$  is finite, the  $\beta$  will decrease with the increase of  $d_2$ . If the  $d_2$  is infinite, the effect of gate-anode distance on  $\beta$  can be ignored. All the results of theoretical calculation can provide useful information in the fabrication and design of the gated nanotube cold cathode for field emission display panels and other nanoscale triode devices. © 2007 American Institute of Physics.

[DOI: [10.1063/1.2818019](https://doi.org/10.1063/1.2818019)]

### I. INTRODUCTION

Carbon nanotubes are of increasing interest due to their remarkable field emission properties for their applications to vacuum nanoelectronic devices.<sup>1-4</sup> Carbon nanotubes are just rolled graphite sheets and have a diameter of the order of nanometer and up to a few micrometers in length. Due to their small diameters and relatively long height, nanotube has a high aspect ratio and thus generates a large electric field enhancement, which would lead to the greater local field at the top of nanotubes. The emission electrons could penetrate the potential barrier into the vacuum with tunnel effect,<sup>5,6</sup> and the higher current density could obtain with a lower voltage. Therefore, carbon nanotubes can be considered to be ideal candidates for the next generation field emitters for flat panel displays, field emission electron source, microwave power amplifiers, and so on.<sup>7-9</sup>

Calculation and simulation for the field emission from carbon nanotubes are mainly concentrated on the individual nanotube<sup>10-15</sup> or several nanotubes without gate electrode.<sup>16-19</sup> Some works have shown that the field emission properties can be influenced by the parameters such as the aspect ratio of nanotube, the anode-cathode distance, vacuum environment, nanotube with open/close caps, gate-hole diameter, etc.<sup>20-24</sup> An important factor in field emission is the relationship between the applied and the local electric field where electron tunneling occurs. The field enhancement factor  $\beta$  is defined as  $\beta = E_a/E_m$ , where  $E_a$  is the actual electric field at the apex of the carbon nanotube and  $E_m$  is the

macroscopic applied electric field. Kokkorakis *et al.*<sup>10,11</sup> reported that the factor  $\beta$  is as a function of  $h/r$  and the enhancement factor of the open nanotube is larger than that of the closed carbon nanotube, where  $h$  is the height of the carbon nanotube and  $r$  is the radius of its cap by the calculation of the field enhancement factor of the open and closed carbon nanotubes with computer simulation. The field enhancement factor of nanotubes array on a planar cathode surface was calculated with model of floating spheres combined with the image charge method by Zhu *et al.*<sup>16</sup> and Wang *et al.*<sup>17-19</sup> The gated nanotube cold cathode is one of the important parts for field emission flat panel displays and other field emission nanotube cold cathode devices;<sup>25-27</sup> the gate-hole radius, spacing between gate and cathode, and applied gate voltage also greatly affected their field emission properties. Using the SIMION 3D 7.0 software and numerical simulation method, Shi and Pi,<sup>24</sup> Nicolaescu *et al.*<sup>28</sup> and Nicolaescu<sup>29</sup> obtained the variation behavior of the field enhancement factor and gate-hole radius, nanotube radial position  $r$  for gated field emission carbon nanotube cold cathode. Although the computer simulation and numerical calculation methods (for solving Laplace equation) were successful in calculating the field distribution and the field enhancement factor in various cases, people also wanted to look for some model systems, which could be solved analytically, with which the trend of the enhancement factor versus various parameters can be easily discussed.

In this paper, the influences of some parameters of triode configurable field emission cold cathode with an individual conductive nanotube as emitter on their field enhancement factor are investigated, in which nanotube is placed in the

<sup>a)</sup> Author to whom correspondence should be addressed. Electronic mail: wangwb@126.com

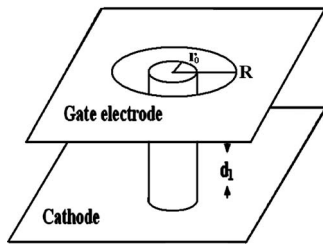


FIG. 1. The model of gated nanotube cold cathode.

center of gate-hole. An ideal model for the field emission cold cathode device is set up. The spatial distributions of the electric potential and the field near the apex of the individual nanotube are analytically calculated on the basis of classical electrostatic theory. The external electric field around the nanotube top surface and enhancement factor are expressed by analytic equations. The field enhancement factor for apex of gated individual nanotube is given as the following expression  $\beta = \lambda + \gamma$ , in which  $\lambda$  and  $\gamma$  are the function of some parameters such as the gate voltage, anode voltage, the geometrical parameters, etc.

## II. MODEL OF THE GATED NANOTUBE COLD CATHODE

For the used model, the conductive single nanotube with opened top operates as the emitter of cold cathode and the nanotube is taken as a conductive hollow cylinder of thin width with small radius, which is vertically placed on cathode plate and in the center of the gate-hole. The geometrical structure sketch of the gated nanotube cold cathode is shown in Fig. 1. In order to simulate the field emission from gated nanotube, we assume that the spacing between the cathode and the gate electrode is  $d_1$ , the diameter of the nanotube outside is  $2r_0$ , which equals to the diameter of the cylindrical tube (the wall thickness of nanotube is ignored). And the distance between the gate electrode and anode is  $d_2$ , the gate-hole radius is  $R$ , the height of the nanotube is  $L$ , which equals to  $d_1$ . Among all the calculation process, the potential of cathode is zero, and the potentials of the anode and gate are  $V_a$  and  $V_g$ , respectively. In our calculation process, the space charge effects, thickness of the gate-electrode, and edge effects of the cathode are neglected and we assumed that the sizes of the all electric plates including anode, cathode, and gate-electrode are much larger than  $r_0$ ,  $R$ ,  $d_1$ ,  $d_2$ , and so on. Therefore, this ideal model mentioned above is rather propitious to the studies of a gated cold cathode with the thin-walled carbon nanotube with opened end as emitters.

## III. CALCULATION FOR FIELD AROUND THE GATED NANOTUBE TOP

### A. Principle of the algorithm

In order to calculate the field and potential distribution, a cylindrical coordinate system is used in this paper shown in Fig. 2. The  $r$ ,  $z$ , and  $\varphi$  are the positions of radial, axial direction, and angle, respectively. The intersected point of the cathode electrode and axes of cylindrical tube was taken as the origin in this study. The electric potential distribution

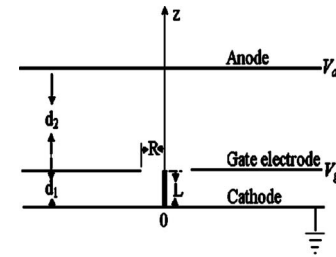


FIG. 2. The calculation model of gated nanotube cold cathode device.

around the nanotube in a triode configuration should be satisfied with Poisson equation, which can be expressed by the equation

$$\nabla^2 \Phi(z, r, \varphi) = \frac{\delta}{\epsilon}, \quad (1)$$

where the  $\delta$ ,  $\epsilon$ , and  $\Phi(z, r, \varphi)$  are the density of space charges, insulation constant of the medium, and the potential of electric distribution, respectively. The boundary conditions of potential distribution near the nanotube in the model of triode structure are as follows:  $\Phi|_{z=0}=0$ ,  $(\partial\Phi/\partial r)|_{z=(d_1+d_2)}=0$ ,  $\Phi|_{z=(d_1+d_2)}=V_a$ ,  $\Phi|_{z=d_1}^{r=R}=V_g$ ,  $\Phi|_{r=r_0}=V_0$  in the region of  $0 \leq z \leq L$ , etc. Since the space charge effects could be ignored, the potential distribution of the triode would be in accord with Laplace equation,

$$\nabla^2 \Phi(z, r, \varphi) = 0. \quad (2)$$

For the potential being symmetrical around the axis of single nanotube in the triode structure, the solutions of the Eq. (2) can be obtained through variable separation method under the conditions of  $k=0$  and  $k>0$ , respectively.

$$\Phi(z, r) = (az + b)(A \ln r + B), \quad (k=0), \quad (3)$$

$$\Phi(z, r) = [a' \exp(kz) + b' \exp(-kz)][A' J_0(kr) + B' N_0(kr)], \quad (k>0), \quad (4)$$

where the  $k$ ,  $a$ ,  $b$ ,  $A$ ,  $B$ ,  $a'$ ,  $b'$ ,  $A'$ , and  $B'$  are all constants, and  $J_0(kr)$  and  $N_0(kr)$  are the Bessel function and Neumann function, respectively.

### B. The electric field over the nanotube top

In our model, the function of  $\Phi(z, r)$  must be the limited values in triode structure, but the two functions of  $\ln(r)$  and  $N_0(kr)$  have the following properties:  $\lim_{r \rightarrow 0} \ln(r) \rightarrow -\infty$ ,  $\lim_{r \rightarrow 0} N_0(kr) \rightarrow -\infty$  in the region of  $L \leq z \leq (d_1 + d_2)$ . Keeping the function of electric potential distribution to be a limited value, it is required  $A=0$  and  $B'=0$  in the above two equations [Eqs. (3) and (4)]. Thus the above Eqs. (3) and (4) must be rewritten as

$$\Phi = az + b, \quad (5)$$

$$\Phi(z, r) = A'[a' \exp(kz) + b' \exp(-kz)]J_0(kr). \quad (6)$$

Considering the boundary conditions  $(\partial\Phi/\partial r)|_{z=(d_1+d_2)}=0$  and  $\Phi|_{z=d_1+d_2}=V_a$ , the function of potential distribution over the top of nanotube may be expressed by the following equation:

$$\Phi(z, r) = V_a - a(d_1 + d_2 - z) + \sum_{i=1}^{\infty} C_i \exp(-k_i z) \{1 - \exp[-2k_i(d_1 + d_2 - z)]\} J_0(k_i r), \quad (7)$$

where  $C_i (i=1, 2, 3, \dots)$  are constants. In view of the properties of Bessel function and the boundary conditions  $\Phi|_{z=d_1}^{r=R} = V_g$  and  $\Phi|_{z=L}^{r=0} = 0$ , the approximate solution of the electric potential distribution of nanotube top can be given by Eq. (8),

$$\begin{aligned} \Phi(z, r) = & V_a - \left\{ \frac{(V_a - V_g)J_0(k_1 r_0) - V_a J_0(k_1 R)}{[J_0(k_1 r_0) - J_0(k_1 R)]d_2} \right\} (d_1 + d_2 \\ & - z) - \left\{ V_a - \frac{(V_a - V_g)J_0(k_1 r_0) - V_a J_0(k_1 R)}{[J_0(k_1 r_0) - J_0(k_1 R)]} \right\} \\ & \times \frac{\exp(-k_1 z) \{1 - \exp[-2k_1(d_1 + d_2 - z)]\}}{\exp(-k_1 d_1) [1 - \exp(-2k_1 d_2)]} J_0(k_1 r). \end{aligned} \quad (8)$$

Therefore, the electric field intensity on the top of the nanotube is obtained from the formula  $-\nabla\Phi(z, r) = E$  of electric potential grads combining with Eq. (8),

$$\begin{aligned} E_r = & -k_1 \left\{ V_a - \frac{(V_a - V_g)J_0(k_1 r_0) - V_a J_0(k_1 R)}{[J_0(k_1 r_0) - J_0(k_1 R)]} \right\} \\ & \times \frac{\exp(-k_1 z) \{1 - \exp[-2k_1(d_1 + d_2 - z)]\}}{\exp(-k_1 d_1) [1 - \exp(-2k_1 d_2)]} J_1(k_1 r), \end{aligned} \quad (9)$$

$$\begin{aligned} E_z = & - \left\{ \frac{(V_a - V_g)J_0(k_1 r_0) - V_a J_0(k_1 R)}{[J_0(k_1 r_0) - J_0(k_1 R)]d_2} \right\} - k_1 \left\{ V_a \right. \\ & \left. - \frac{(V_a - V_g)J_0(k_1 r_0) - V_a J_0(k_1 R)}{[J_0(k_1 r_0) - J_0(k_1 R)]} \right\} \\ & \times \frac{\exp(-k_1 z) \{1 + \exp[-2k_1(d_1 + d_2 - z)]\}}{\exp(-k_1 d_1) [1 - \exp(-2k_1 d_2)]} J_0(k_1 r). \end{aligned} \quad (10)$$

The  $E_r$  and  $E_z$  are denoted to the electric field intensities of radial direction and axial direction, respectively.

### C. The electric field around the nanotube outside

Under the conditions of  $0 \leq z \leq L$  and  $r_0 \leq r$  in the triode model, considering the boundary conditions including  $\Phi|_{z=0} = 0$  and  $\Phi|_{r=r_0} = 0$ , the function of electric potential distribution can be expressed as the following equation:

$$\Phi(z, r) = \sum_{i=1}^{\infty} A_i'' \operatorname{sh}(k_i z) \left[ J_0(k_i r) - \frac{J_0(k_i r_0)}{N_0(k_i r_0)} N_0(k_i r) \right], \quad (11)$$

where  $A_i'' (i=1, 2, 3, \dots)$  are constants. We assumed that  $\Phi(L, r)$  is a composite function of the Bessel functions  $J_0(k_1 r)$  and  $N_0(k_1 r)$ , namely,  $\Phi(L, r) = U_m [J_0(k_1 r) - J_0(k_1 r_0) N_0(k_1 r) / N_0(k_1 r_0)]$  at  $z=L$ , where the  $U_m$  is a constant and is equal to the electric potential at the center of the circular gate-hole when without nanotube. As the gate-hole radius is not too large [i.e., under the condition of  $R$

$\leq \pi d_1 d_2 / (d_1 + d_2)$ ],  $U_m$  may be described by  $V_g + R[(V_a - V_g) / d_2 - V_g / d_1] / \pi$  with Scherzer formula.<sup>30</sup> However, if the  $R$  is much larger than  $d_1$ , the constant  $U_m$  will be approximately equaled to the  $V_a d_1 / (d_1 + d_2)$ . Therefore, the following equations  $A_i'' = U_m / \operatorname{sh}(k_i L)$ ,  $A_i'' = 0$  ( $i=2, 3, 4, \dots$ ) are obtained from the Eq. (11), and the function of electric potential distribution is rewritten as follows:

$$\Phi(z, r) = U_m \frac{\operatorname{sh}(k_1 z)}{\operatorname{sh}(k_1 L)} \left[ J_0(k_1 r) - \frac{J_0(k_1 r_0) N_0(k_1 r)}{N_0(k_1 r_0)} \right]. \quad (12)$$

Thus the corresponding electric field intensities can be obtained as follows:

$$E_z = -k_1 U_m \frac{\operatorname{sh}(k_1 z)}{\operatorname{sh}(k_1 L)} \left[ J_0(k_1 r) - \frac{J_0(k_1 r_0) N_0(k_1 r)}{N_0(k_1 r_0)} \right], \quad (13)$$

$$E_r = k_1 U_m \frac{\operatorname{sh}(k_1 z)}{\operatorname{sh}(k_1 L)} \left[ J_1(k_1 r) - \frac{J_0(k_1 r_0) N_1(k_1 r)}{N_0(k_1 r_0)} \right], \quad (14)$$

where  $E_r$  and  $E_z$  are the electric field intensities of radial direction and axial direction, respectively.

In addition, the following relationship is also obtained from Eq. (12) with the boundary condition  $\Phi|_{z=d_1}^{r=R} = V_g$  due to the height of nanotube equals the spacing of cathode to gate electrode in this paper,

$$\begin{aligned} V_g N_0(k_1 r_0) / [N_0(k_1 r_0) J_0(k_1 R) - J_0(k_1 r_0) N_0(k_1 R)] = & V_g \\ & + R[(V_a - V_g) / d_2 - V_g / L] / \pi. \end{aligned}$$

So,  $k_1$  can be determined by equation above.

## IV. CALCULATION FOR FIELD ENHANCEMENT FACTOR

In order to compute the enhancement factor, the actual electric field at the end of nanotube is calculated from Eq. (14) at the conditions of  $r=r_0$  and  $z=L$ . The actual electric field could be expressed as

$$E_a = \lambda' V_g + \gamma' V_a, \quad (15)$$

where  $\lambda' = k_1 [1 - R(L + d_2) / \pi L d_2] [J_1(k_1 r_0) - J_0(k_1 r_0) N_1(k_1 r_0) / N_0(k_1 r_0)]$  and  $\gamma' = k_1 R / \pi d_2 [J_1(k_1 r_0) - J_0(k_1 r_0) N_1(k_1 r_0) / N_0(k_1 r_0)]$ , respectively. Namely, the  $\lambda'$  and  $\gamma'$  are as the function of gate-hole radius  $R$ , nanotube radius  $r_0$ , gate-anode distance  $d_2$ , nanotube height  $L$ , gate voltage, the anode voltage, etc. The calculated result in Eq. (15) is in accordance with equation of  $E_a$  in Ref. 29.

For the above calculation model, the macroscopic electric field can be expressed as  $E_m = V_a / (d_1 + d_2)$  when gate voltage is zero, which is considered as the corresponding macroscopic electric field of gated structure in this study. Thus the field enhancement factor was determined with the formula  $\beta = E_a / E_m$ ,

$$\beta = \lambda + \gamma, \quad (16)$$

where  $\lambda = \lambda' (d_2 + L) V_g / V_a$  and  $\gamma = (d_2 + L) \gamma'$ , respectively.

## V. RESULTS AND DISCUSSION

Figure 3 shows the equipotential lines for gated open nanotube with different gate-hole radii and nanotube radii

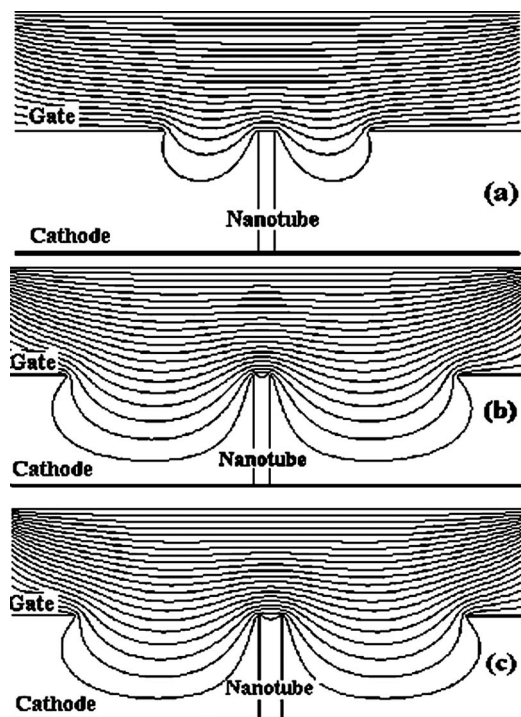


FIG. 3. The equipotential lines for gated open nanotubes with different gate-hole radii and nanotube radii when applied gate voltage is zero.

when the gate voltage is zero. The equipotential lines for the model with same nanotube size and different gate-hole radii are shown in Figs. 3(a) and 3(b), and the equipotential lines for the same gate-hole radii and different radii of nanotube with the same heights are shown in Figs. 3(b) and 3(c). We can see that the equipotential lines and field penetrated into a greater extent between the gate and cathode for the gated open nanotube cold cathode with larger gate-hole radius. It indicates that the corresponding enhancement factor is larger for the gate-hole with larger radius when gate voltage is zero because the screening effect of gated electrode for the field around the nanotube is weak in this instance.

The variation of enhancement factor versus gate-hole radius at  $V_a=1000$  V,  $V_g=100$  V,  $L=10$   $\mu\text{m}$ ,  $d_2=200$   $\mu\text{m}$ ,  $r_0=0.02$   $\mu\text{m}$  is shown in Fig. 4(a). The result shows that the enhancement factor increases rapidly with the decrease of the gate radius, which is in accordance with the result of Ref. 28.

However, the field enhancement factor should be described by following equation when the gate voltage is zero:

$$\beta = k_1 l [J_1(k_1 r_0) - J_0(k_1 r_0) N_1(k_1 r_0) / N_0(k_1 r_0)], \quad (17)$$

where  $l$  is the effective length of nanotube. When  $R$  is not much larger than  $L$  [in the region of  $R \leq \pi L d_2 / (L + d_2)$ ], the  $l$  should be equaled to  $R(1 + L/d_2) / \pi$ . So the enhancement factor can be rewritten as  $\beta = \gamma$ , which is the same as the result obtained from Eq. (16) when the gate voltage is zero. However, if the gate-hole radius  $R$  is much larger than nanotube height  $L$ , the  $l$  will be equaled to the nanotube height  $L$  because the electric field screening effect of gate electrode for the field around the nanotube is very small, and the penetrated fields of under the gate-hole are largest for the gated nanotube cold cathode with enough large gate-hole radius, when the gate voltage is zero.

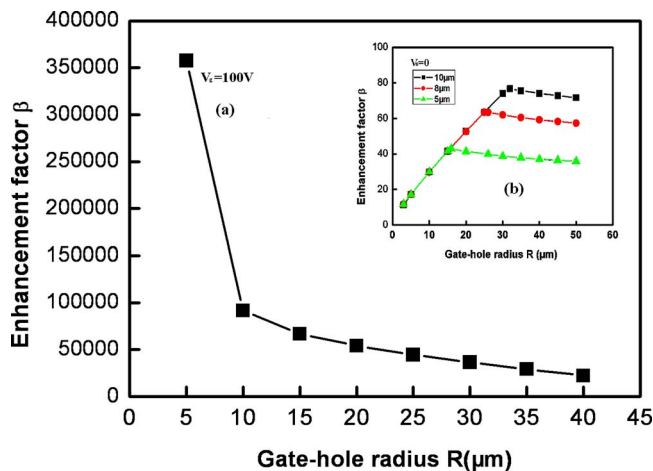


FIG. 4. (Color online) The plots of field enhancement factor as a function of gate-hole radius; (a) shows the variation of  $\beta$  vs  $R$  at  $V_a=1000$  V,  $V_g=100$  V,  $L=10$   $\mu\text{m}$ ,  $d_2=200$   $\mu\text{m}$ ,  $r_0=0.02$   $\mu\text{m}$  and (b) shows the variation of  $\beta$  vs  $R$  when the gate-anode distance is infinite at different nanotube heights of 0.01, 0.02, and 0.03  $\mu\text{m}$ , and  $V_g=0$ , respectively.

Furthermore, we also compute the field enhancement factor for the different gate-hole radii of model with different nanotube heights ( $L=10, 8, 5$   $\mu\text{m}$ ) at  $r_0=0.02$   $\mu\text{m}$ ,  $V_g=0$ , and the corresponding variation curves for the field enhancement factors as a function of gate-hole radius are shown in Fig. 4(b). However, the solution results show that the enhancement factor increases with the increase of the gate-hole radius under the conditions of  $R < \pi L$  and the infinite gate-anode distance (which is much larger than nanotube height) at  $V_g=0$  because the gate voltage effect for enhancement of field is not main and the gate electrode has some electric field screening effect for the field around the nanotube. When the  $R$  is larger than  $\pi L$ , the  $\beta$  is close to the maximum of the enhancement factor, which increases with the nanotube height due to the small electric screening effect in this instance.

Figure 5 shows the enhancement factor  $\beta$  as a function of nanotube radius when the gate-anode distance is infinite at the conditions of  $L=20$   $\mu\text{m}$  and  $R=60$   $\mu\text{m}$ . The enhancement factor decreases rapidly with the increase of nanotube

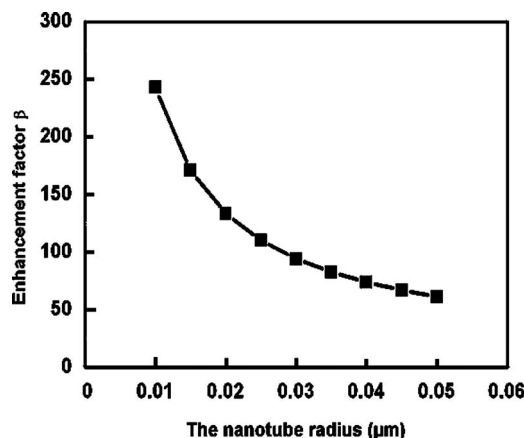


FIG. 5. The variation of enhancement factor  $\beta$  vs nanotube radius when the gate-anode distance is infinite at  $L=20$   $\mu\text{m}$ ,  $R=60$   $\mu\text{m}$ .

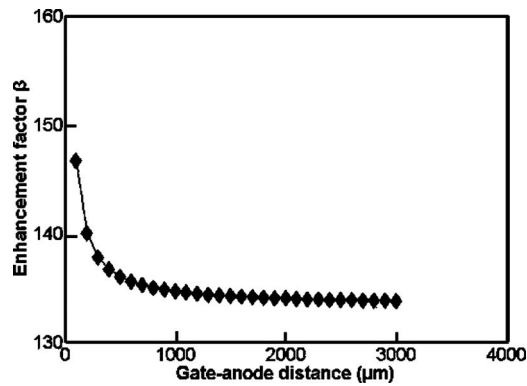


FIG. 6. The variation of enhancement factor  $\beta$  vs gate-anode distance at the  $r_0=0.01 \mu\text{m}$ ,  $d_1=10 \mu\text{m}$ , and  $R=30 \mu\text{m}$ , respectively.

radius, and its variation law is almost in accordance with the calculation and simulation results of diode configuration and experiment.<sup>10–15</sup>

The influence of anode-cathode distance on field enhancement factor of individual nanotube and several nanotubes array for planar cathode was reported by Wang *et al.*<sup>17–19</sup> The simulation results showed that the enhancement factor decreased with the increase of the anode-cathode distance when the anode-cathode distance was not much larger than the nanotube height. However, when the anode-cathode distance is infinite, the effect of anode-cathode distance on enhancement factor is very weak in the model of diode structure. In our paper, the variation of enhancement factor  $\beta$  versus gate-anode distance  $d_2$  under the conditions of  $r_0=0.01 \mu\text{m}$ ,  $d_1=10 \mu\text{m}$ , and  $R=30 \mu\text{m}$  is shown in Fig. 6. The effect of  $d_2$  on the factor is very weak, which is compared to the effect of  $r_0$  and  $R$ , although the enhancement factor will increase a little when the gate-anode distance is less than the spacing of  $500 \mu\text{m}$ . The overall effect of  $d_2$  on the enhancement factor is weak, therefore  $\beta$  can be considered as a constant when  $d_2$  is larger than  $500 \mu\text{m}$ . At the threshold voltage of field emission, the field strength  $E$  at the top is fixed. From the expression of  $E=\beta V_a/(d_1+d_2)$ , we see that one should make  $d_2$  smaller in order to get lower threshold voltage.

## VI. CONCLUSIONS

The field enhancement factor of gated nanotube with opened top was analytically calculated by the electrostatic method in this paper. These consequences above are almost consistent with the simulation results for enhancement factor of nanotube in diode and triode structures. Therefore, the theoretical calculation results could provide useful information for the fabrication and design of the gated nanotube cold cathode field emission display panels and other nanoscale triode devices.

## ACKNOWLEDGMENTS

The authors gratefully acknowledge the financial supports from the National Natural Science Foundation of China (Grant Nos. 50072029 and 50572101).

- <sup>1</sup>W. I. Milne, K. B. K. Teo, M. Chhowalla, G. A. J. Amaratunga, D. Pribat, P. Legagneux, G. Pirio, V. T. Binh, and V. Semet, *Curr. Appl. Phys.* **2**, 509 (2002).
- <sup>2</sup>K. B. K. Teo, M. Chhowalla, G. A. J. Amaratunga, W. I. Milne, P. Legagneux, G. Pirio, L. Gangloff, D. Pribat, W. H. Bruenger, J. Eichholz, H. Hanssen, D. Friedrich, S. B. Lee, D. G. Hasko, and H. Ahmed, *J. Vac. Sci. Technol. B* **20**, 116 (2002).
- <sup>3</sup>W. Zhua, C. Bower, O. Zhou, G. Kochanski, and S. Jin, *Appl. Phys. Lett.* **75**, 873 (1999).
- <sup>4</sup>G. Pirio, P. Legagneux, D. Pribat, K. B. K. Teo, M. Chhowalla, G. A. J. Amaratunga, and W. I. Milne, *Nanotechnology* **13**, 1 (2002).
- <sup>5</sup>P. N. Minh, L. T. T. Tuyen, T. Ono, H. Miyashita, Y. Suzuki, H. Mimura, and M. Esashi, *J. Vac. Sci. Technol. B* **21**, 1705 (2003).
- <sup>6</sup>J. H. Choi, S. H. Choi, J. H. Han, J. B. Yoo, C. Y. Park, T. Jung, S. G. Yu, I. T. Han, and J. M. Kin, *J. Appl. Phys.* **94**, 487 (2003).
- <sup>7</sup>W. A. D. Heer, A. Châtelain, and D. Ugarte, *Science* **270**, 1179 (1995).
- <sup>8</sup>P. G. Collins and A. Zettl, *Phys. Rev. B* **55**, 9391 (1997).
- <sup>9</sup>K. B. K. Teo, M. Chhowalla, G. A. Amaratunga, W. I. Milne, G. Pirio, P. Legagneux, D. Pribat, and D. G. Hasko, *Appl. Phys. Lett.* **80**, 2011 (2002).
- <sup>10</sup>G. C. Kokkorakis, A. Modinos, and J. P. Xanthakis, *J. Appl. Phys.* **91**, 4580 (2002).
- <sup>11</sup>G. C. Kokkorakis, J. A. Roumeliotis, and J. P. Xanthakis, *J. Appl. Phys.* **95**, 1468 (2004).
- <sup>12</sup>X. Zheng, G. H. Chen, Z. Li, S. Deng, and N. Xu, *Phys. Rev. Lett.* **92**, 106803 (2004).
- <sup>13</sup>A. Buldum and J. P. Lu, *Phys. Rev. Lett.* **91**, 236801 (2003).
- <sup>14</sup>L. Nilsson, O. Groening, C. Emmenegger, O. Kuettel, E. Schaller, L. Schlapbach, H. Kind, J. M. Bonard, and K. Kem, *Appl. Phys. Lett.* **76**, 2071 (2000).
- <sup>15</sup>X. Q. Wang, M. Wang, P. M. He, Y. B. Xu, and Z. H. Li, *J. Appl. Phys.* **96**, 6752 (2004).
- <sup>16</sup>Z. B. Zhu, W. L. Wang, and K. J. Liao, *Proc. SPIE* **4918**, 145 (2002).
- <sup>17</sup>X. Q. Wang, Y. B. Xu, H. L. Ge, and M. Wang, *Diamond Relat. Mater.* **15**, 1565 (2006).
- <sup>18</sup>X. Q. Wang, M. Wang, Z. H. Li, Y. B. Xu, and P. M. He, *Ultramicroscopy* **102**, 181 (2005).
- <sup>19</sup>M. Wang, Z. H. Li, X. F. Shang, X. Q. Wang, and Y. B. Xu, *J. Appl. Phys.* **98**, 014315 (2005).
- <sup>20</sup>Y. Saito, K. Hamaguchi, R. Mizushima, S. Uemura, T. Nagasako, J. Yotani, and T. Shimojo, *Appl. Surf. Sci.* **146**, 305 (1999).
- <sup>21</sup>Y. Saito, *Ultramicroscopy* **73**, 1 (1998).
- <sup>22</sup>Y. Chen, D. T. Shaw, and L. Guo, *Appl. Phys. Lett.* **76**, 2469 (2000).
- <sup>23</sup>L. Nilsson, O. Gröning, P. Gröning, O. Kuttel, and L. Schlapbach, *Thin Solid Films* **383**, 78 (2001).
- <sup>24</sup>N. Shi and D. F. Pi, *Proc. SPIE* **4600**, 196 (2001).
- <sup>25</sup>S. H. Lim, H. S. Yoon, J. H. Moon, K. C. Park, and J. Jang, *Appl. Phys. Lett.* **87**, 243106 (2005).
- <sup>26</sup>J. C. Shi, S. Z. Deng, N. S. Xu, R. H. Yao, and J. Chen, *Appl. Phys. Lett.* **88**, 013112 (2006).
- <sup>27</sup>Y. M. Wong, W. P. Kang, J. L. Davidson, B. K. Choi, W. Hofmeister, and J. H. Huang, *Diamond Relat. Mater.* **14**, 2069 (2005).
- <sup>28</sup>D. Nicolaescu, M. Nagao, V. Filip, S. Kanemara, and J. Itoh, *Jpn. J. Appl. Phys., Part 1* **44**, 3854 (2005).
- <sup>29</sup>D. Nicolaescu, *J. Vac. Sci. Technol. B* **13**, 531 (1995).
- <sup>30</sup>G. J. Zhao, B. J. Ling, and S. X. Xue, *Electric Optics* (National Defence Industry, ChengDu, 1985), p. 262.